power transported by the waves, averaged over a period, is equal to

$$\frac{1}{4K\tau}\int_{-2K\tau}^{+2K\tau}\frac{c}{8\pi}\mathcal{E}^2(z,t)dt=\frac{c}{8\pi}\mathcal{E}_0^2\left\{\frac{E(K(\lambda))}{K(\lambda)}+(\lambda^2-1)\right\}. \tag{18}$$

The reciprocal velocity of the modulation amplitude is given by

$$\frac{1}{v}=\frac{\eta}{c}+\frac{2\pi N\omega\mu^2\tau^2}{\hbar c\eta}\int_{-\infty}^{\infty}\frac{g(\Delta)d\Delta}{[(1-\Delta^2\tau^2)^2+4\Delta^2\tau^2\lambda^2]^{1/2}}. \tag{19}$$

The solutions presented above[8] correspond to a simple undamped model. In a real solid, relaxation effects would interfere with the coherent absorption and emission of radiation which is necessary for distortionless propagation of light. In order to observe the propagation effects described here, it would be necessary to have relaxation times long compared with the period of the amplitude-modulation function. From Eq. (9) and the definition of τ it is seen that rapid amplitude modulation can be achieved in the presence of strong fields $\mathcal{E}_0=2\hbar/\mu\tau$.

I wish to thank Professor S. R. Hartmann for several helpful and stimulating discussions.

*Work supported wholly by the Joint Services Electronics Program (U.S. Army, U.S. Navy, and U.S. Air Force) under Contract No. DA-28-043 AMC-00099 (E).

[1]J. D. Jackson, Classical Electrodynamics (John Wiley & Sons, Inc., New York, 1963), Sec. 6.10.

[2]R. Feynman, F. Vernon, and R. Hellwarth, J. Appl. Phys. 28, 49 (1957).

[3]S. L. McCall and E. L. Hahn, Phys. Rev. (to be published). In this paper it is mentioned that there are two other classes of solutions related to the hyperbolic secant.

[4]P. Bryd, Handbook of Elliptic Integrals (Lange, Maxwell & Springer Ltd., New York, 1954). The amplitude modulation function shown in Eq. (8a) has also been found by F. T. Arecchi, V. DeGiorgio, and S. G. Someda [Phys. Letters 27A 588 (1968)].

[5]G. B. Hocker and C. L. Tang, Phys. Rev. Letters 21, 591 (1968).

[6]S. L. McCall and E. L. Hahn, Phys. Rev. Letters 18, 908 (1967).

[7]S. R. Hartmann and E. L. Hahn, Phys. Rev. 128, 2042 (1962).

[8]Professor E. T. Jaynes (private communication) has found additional solutions to the equations.

DETECTION OF SINGLE QUANTIZED VORTEX LINES IN ROTATING He II*

Richard E. Packard and T. M. Sanders, Jr.
H. M. Randall Laboratory of Physics, University of Michigan, Ann Arbor, Michigan 48104
(Received 10 March 1969)

We have utilized the trapping of electrons on quantized vortex lines in rotating He II to permit detection of single lines in order to study the appearance and disappearance of the first few lines in a capillary rotating about its axis. It seems likely that an extension of the method will permit study of the spatial distribution of vortices in rotating vessels of He II.

It is widely believed that superfluid velocity fields are irrotational everywhere except at singular lines around which the circulation is quantized in units of Planck's constant divided by m, the mass of a helium atom.[1] For a cylindrical bucket of helium, rotating about its symmetry axis, theory[2] predicts that as the angular velocity ω is raised from zero, the helium should remain at rest until a first critical angular velocity (which depends on the bucket radius R) is reached. Above this, the equilibrium state of the system has a single vortex line along the axis; at higher angular velocities more vortices appear. When their number N is large it approaches $\omega mR^2/\hbar$.

The most successful experiment carried out under conditions where only a few vortices should be present is probably that of Hess and Fairbank.[3] They verified one prediction of the vortex picture by finding the angular momentum of a rotating capillary to be lower than that corresponding to rigid-body rotation. They did not, however, resolve any step structure associated with the appearance of single vortices. In rotating He II electrons become trapped on structures which inhibit their motion perpendicular to the axis of rotation but which allow them to be mobile paral-

lel to the axis. This has been interpreted successfully in terms of the quantized vortex picture of rotating helium.[4-7] These experiments have involved trapping approximately 10^3 electrons/line in vessels containing 10^3 to 10^4 lines.

Since our object was to detect single lines, we conducted exploratory experiments to see if the trapped electrons could be extracted from the liquid, after which a sensitive particle detector could be used. After charging the lines from a radioactive source, we found virtually the same charge released either to a collector immersed in the liquid or to one in the vapor above the liquid. (This was true in spite of the fact that untrapped charge encounters increasing difficulty in passing out of the liquid as the temperature is lowered.[8]) We decided to explore the possibility of using a counter filled with helium vapor to detect the charge from a single line. We found that we were able to make stable proportional counters with gains[9] of approximately 50; these were used in the experiments which we will describe below.

All the experiments were carried out near 1.25 K in a rotating cryostat supported on an air bearing. Low-level electronics, various power supplies, and a bath-temperature regulator are located on the rotating table. Electrical leads pass between the lab and the rotating system through mercury slip rings.

The experimental cell shown in Fig. 1 is a bucket made by drilling a 1-mm-diam hole down the common axis of four cylindrical pieces of resistance material (taken from Allen-Bradley 100-kΩ 2-W resistors). Electric fields are produced along the axis of the capillary by applying bias voltages to the metalized ends of the sections. The vessel contains a flat tritiated-titanium β source at the bottom and opens directly into a proportional counter at the top. A surrounding glass-walled can is filled from the He II bath by use of a valve. The liquid meniscus is set midway up the top section, as shown in Fig. 1, and remains stable for the duration of a run.

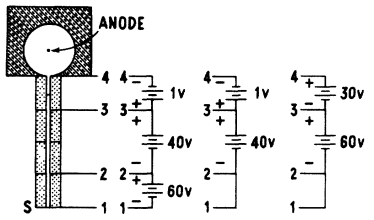

FIG. 1. The experimental cell and the applied voltages for the charging, clearing, and collecting parts of the cycle, respectively. S is the β source; the diameter of the capillary is 1 mm and the length approximately 3 cm. The meniscus is shown between electrodes 3 and 4.

We detect the vortex lines in a cycle which is repeated once every 30 sec. In the first (charging) part of the cycle, an electric field is applied which sweeps electrons away from the radioactive source and draws them along the axis of the bucket. As the electrons move through the liquid, some of them are trapped on any vortex lines which are present; the remaining charge is collected at the walls near the top section, where a slight repelling field exists. After charging in this manner for about 27 sec, the field in front of the source is turned off so that no more charge leaves the source region. This clearing configuration is maintained for 2 sec to allow all untrapped charge to be collected at the walls. Finally a field is applied which pulls the trapped charge up to the meniscus where it is extracted from the liquid and enters the proportional counter, whose anode current is integrated in an operational amplifier (Analog Devices Model No. 301) providing a pulse proportional to the total charge collected. This output is filtered and recorded both in analog and digital (printed) form. Transitions between different numbers of lines should appear as steplike changes in the pulse height. After the charge is collected the biases are returned to the charging configuration. This cycle repeats automatically while the vessel is slowly accelerated from rest to approximately 2 rad/sec and then decelerated to rest at the same rate. A complete run takes about 10 h.

Figure 2(a) shows raw data, not averaged or adjusted in any way, taken during the acceleration half of one run. We believe the following features to be significant:

(1) There is no detectable signal until the first obvious step appears.

(2) There is a series of steps of approximately equal size.

(3) The steps occur at angular velocities comparable with those where theory predicts new vortices should appear; for example, the first step appears at 1.6 rad/sec; theory predicts one vortex line would be stable at 1 rad/sec. We interpret each step as the appearance of a single vortex line. The deceleration half of this run is not shown because we ran out of helium in the Dewar.

The acceleration half of a subsequent run [Fig.

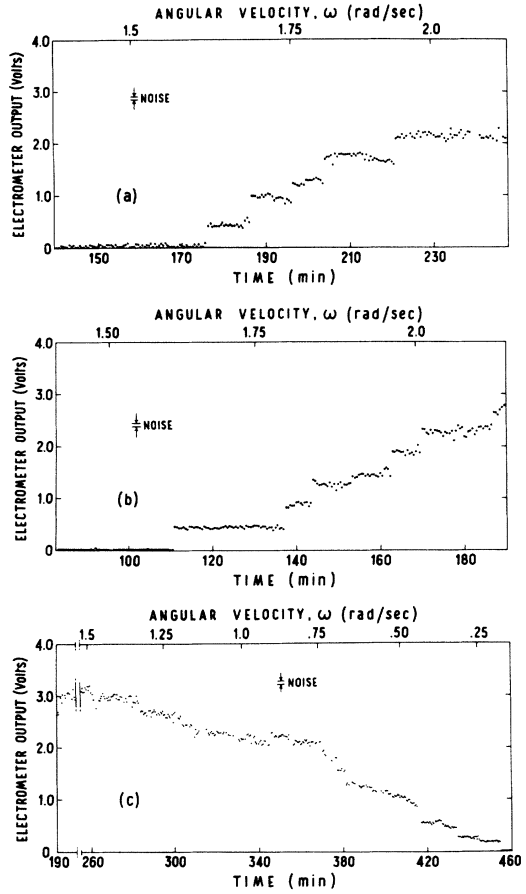

FIG. 2. Collected charge versus time. (a) and (b) Data taken during an acceleration. (c) Data taken during deceleration. Time is measured from the beginning of rotation. 1 V of electrometer output is equivalent to approximately 6×10^{-14} C.

2(b)] resembles the first one closely. The first step occurs at the same angular velocity as in Fig. 2(a); subsequent steps appear at different, but comparable, values.

However, characteristically different behavior is seen during deceleration [Fig. 2(c)]: A large signal persists down to angular velocities where no signal existed during acceleration; there are large signal fluctuations, a gradual decrease in signal, and occasional discontinuous downward steps. Incidentally, the absence of fluctuations at the baseline signal level in Figs. 2(b) and 2(c) is spurious, since the pulse-height recording system only responds to positive signals and the quiescent electrometer output was slightly negative during this run.

We can understand most of the qualitative features of the data in terms of the theory,[2] which assumes that the stable and metastable distributions of vortices are those which minimize the quantity $E'=E-\omega L$. Here E is the kinetic energy of the superfluid and L its angular momentum. At any angular velocity there is a unique number (and distribution) of vortices which minimizes E'; there can, however, be metastable minima for distributions containing other numbers of vortices. There is, furthermore, always a barrier to be overcome when a vortex passes from the wall, where it is presumably created, into the interior, where its stable position lies.

For example, when $\omega < \hbar/mR^2$ the only stable state is one of no vortices. For $\hbar/mR^2 < \omega < (\hbar/mR^2)\ln(R/a)$, E' has a local minimum with a vortex line on the axis, but this value of E' is greater than that corresponding to no vortices, making a single vortex on the axis metastable. [a is the vortex core radius; for our apparatus $\ln(R/a)=15.4$.] For $\omega > (\hbar/mR^2)\ln(R/a) \cong 1$ rad/sec, E' is lower with a vortex on the axis than with no vortices, but the vortex-free state could be metastable. Similar, but more complicated, situations occur with larger numbers of vortices. We believe that the characteristic hysteresis we observe is due to these effects. As the vessel is accelerated from rest, the first vortex appears not when it would first be stable, but when the barriers are sufficiently low so that fluctuations can carry the system to the one-vortex state. Similarly, upon deceleration the one-vortex state persists beyond the point where it might be energetically favorable for it to decay. We do not know what type of fluctuation is important in the experiment, but we suspect macroscopic vibrations of the apparatus.

We conclude by remarking on some limitations of the present experiment. First, it does not count the number of vortices at an instant, but measures behavior over a 30-sec period. Fluctuations in the vortex configuration will certainly complicate our data. Second, we have not taken any great pains to insure that the axis of rotation coincides with that of the capillary. It is easy to show that a relative displacement of the axes would not be important, but the effects of an angular misalignment are unknown. We have not yet studied the effect of changing the temperature, angular acceleration, or capillary radius.

We are pursuing the possibility that at lower temperatures, where the vapor density is low, extraction of charge from the end of the lines at the meniscus could be utilized to "take a picture" of the spatial distribution of lines by focusing the electrons onto a phosphor or photographic plate.

*Work supported in part by the U. S. Atomic Energy Commission.

[1]Both experimental and theoretical developments are reviewed in J. Wilks, The Properties of Liquid and Solid Helium (Clarendon Press, Oxford, England, 1967), Chaps. 12 and 13; or E. L. Andronikashvili and Yu. G. Mamaladze, Rev. Mod. Phys. 38, 567 (1966).

[2]G. B. Hess, Phys. Rev. 161, 189 (1967).

[3]G. B. Hess and W. M. Fairbank, Phys. Rev. Letters 19, 216 (1967).

[4]G. Careri, W. D. McCormick, and F. Scaramuzzi, Phys. Letters 1, 61 (1962).

[5]R. J. Donnelly, Experimental Superfluidity (University of Chicago Press, Chicago, Ill., 1967), Chap. 6.

[6]R. L. Douglass, Phys. Rev. 141, 192 (1966).

[7]W. P. Pratt, Jr., and W. Zimmermann, Jr., Phys. Rev. 177, 412 (1969).

[8]L. Bruschi, B. Maraviglia, and F. E. Moss, Phys. Rev. Letters 17, 682 (1966).

[9]This is only an estimate. We have not made precise gain measurements.

NONLINEAR DECAY INSTABILITY AND PARAMETRIC AMPLIFICATION OF CYCLOTRON-HARMONIC PLASMA WAVES*

M. Porkolab and R. P. H. Chang
Plasma Physics Laboratory, Princeton University, Princeton, New Jersey 08540
(Received 4 March 1969)

Experimental observation of the resonant mode-mode coupling type of nonlinear decay instability and parametric amplification of cyclotron-harmonic waves is reported. The instability is due to the scattering of finite amplitude waves.

We report experimental observation of (1) nonlinear decay instability of cyclotron-harmonic plasma waves (CHW—or Bernstein modes[1]) when an rf signal (pump) above a threshold level is applied to a probe immersed in a plasma in a magnetic field and (2) parametric amplification of an additional, externally applied rf signal when the pump signal is below threshold level. By nonlinear decay instability we mean the scattering of a finite amplitude wave into other modes which grow exponentially as the initial wave decays. We recall that CHW are quasielectrostatic waves which propagate perpendicularly to a magnetic field,[1] with frequencies in the vicinity of the fundamental and harmonics of the cyclotron frequency. Detailed measurements of wave propagation suggest that the instability we observe is due to decay-type resonant mode-mode coupling of high-frequency traveling CHW, and thus it is different from experiments where the simultaneous emission of both high-frequency and low-frequency signals was observed when the plasma was subjected to intense microwave radiation.[2,3] Although parametric excitation of high-frequency signals has been reported recently when the plasma was subjected to microwave radiation, in these experiments the modes responsible for the interaction were believed to be, although not clearly identified, standing waves in regions with strong density gradients (Buchsbaum-Hasegawa modes).[4] We note that because of possible application to amplifiers, the traveling-wave type of parametric phenomenon is of considerable interest.[5]

The interaction we consider is the decay of a single CHW with frequency ω_0 into two (or more) other CHW with frequencies ω_1, ω_2 by the mechanism of resonant mode-mode coupling, namely,

$$\omega_0(\vec{k}_0) \rightarrow \omega_1(\vec{k}_1) + \omega_2(\vec{k}_2), \tag{1}$$

where

$$\vec{k}_0 = \vec{k}_1 + \vec{k}_2.$$

It has been recently predicted by theory that such a decay process of CHW can be unstable, i.e., the decay modes ω_1, ω_2 can grow exponentially.[6] The energy for the growth is supplied by the decaying pump wave. This process is essentially the inverse of the resonant scattering of CHW observed recently by the present authors[7] (although no instability in the present sense was involved in the latter case).

The experiments were carried out in a hot-cathode helium discharge in a magnetic field (PIG configuration) which was better than 1% uniform. The plasma parameters are as follows: background pressure $\sim 2\times 10^{-3}$ Torr, electron density $n_e \sim 4\times 10^{9}$-1×10^{10} cm^{-3}, electron temperature $T_e \sim 4.5$ eV, and collision frequency of electrons with electrons or with neutrals $\nu_e/\omega \lesssim 10^{-3}$. Three coaxial probes, which were movable radially, were employed for injecting or detecting signals. The probes were provided with 4.0-cm-long T-shaped antennas with the antenna

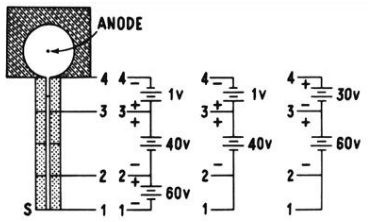

FIG. 1. The experimental cell and the applied voltages for the charging, clearing, and collecting parts of the cycle, respectively. S is the β source; the diameter of the capillary is 1 mm and the length approximately 3 cm. The meniscus is shown between electrodes 3 and 4.